NRL Memorandum Report 1524

FRACTURE ANALYSIS OF A C-141 LANDING GEAR CYLINDER

C. D. BEACHEM

METALLURGY DIVISION

APRIL 1964

U. S. NAVAL RESEARCH LABORATORY
Washington, D.C.

CONTENTS

PROBLEM STATUS

This completes the work on one task of the problem. Work on other tasks is continuing.

AUTHORIZATION

NRL PROBLEM NUMBER: MOL-08

BUREAU PROJECT NUMBER: BRMA 02-091/652-1/R007-06-01

INTRODUCTION

The fracture surface portion of a broken outer cylinder of a nose landing gear that was manufactured for use in the C-141 but broken in the laboratory was delivered to NRL for fracture analysis on 16 January 1964 by Mr. W. P. Whiton of the Marietta Division of the Lockheed Aircraft Corporation.

According to Mr. Whiton and Mr. Brad Ward (ASD, W-PAFB) the cylinder was of AISI 4340 steel, hardened and tempered to produce an ultimate tensile strength of 260-280 KSI. It had been chromium plated during its production and was tested at Lewis Research Center in high-stress low-cycle fatigue by loading it to its calculated UTS (monitored by strain gages) and then releasing the load before reloading. The cylinder broke on the fourth load application at a calculated stress of 160 KSI.

It was requested that NRL establish the causes for the fracture. Mr. Whiton also delivered some fractured low-cycle smooth bar 4340 fatigue specimens from NASA Lewis Laboratories (broken by Mr. Manson's group at that installation) for NRL to try to find fracture surface topographic features that could be related to the cyclic stressing.

According to Mr. Whiton, the piece of cylinder that was delivered to NRL had been chemically treated to remove the chromium plating after the cylinder was broken.

OBSERVATIONS

The cylinder is shown in Figs. 1 and 2 with arrows locating the fracture origin (courtesy of Mr. Whiton). The fracture origin is shown at a higher magnification in Fig. 3. A small shallow surface crack which initiated the fracture is shown between the two vertical arrows. Several small flat-topped hills and flat-bottomed holes are indicated by the other arrows. These were found only near the fracture origin.

Arrows in Fig. 4 show examples of similar raised portions and holes in one of the NASA low-cycle fatigue specimen fracture surfaces.

When the cylinder fracture surface was cleaned with acetone it was found that numerous, deep, fine cracks were present in the cylinder (Fig. 5). These cracks were quite long and in many instances extended completely through the thickness of the cylinder wall. They frequently intersected the primary fracture surface but no shear lips were found at these intersections. Mr. Whiton said that these cracks had been found earlier after the chromium stripping operation.

Cellulose acetate replicas of the fracture surfaces of the outer cylinder and one of the NASA low cycle fatigue specimens were made and these were used to prepare palladium-shadowed carbon replicas for examination in the electron microscope.

Replicas of the fracture initiation region of the cylinder showed the following zones of fracture surface features, starting at the outer surface of the cylinder: (1) burnishing markings at the outer surface of the cylinder, (2) almost totally intergranular facets, (3) mixed dimples and intergranular facets, and (4) isolated patches of completely intergranular facets located within the mixed dimples - intergranular region and within about 1/8-inch of the outer surface of the cylinder at the fracture origin. The remainder of the fracture was mixed intergranular facets and dimples.

The burnishing markings extended about two or three thousandths of an inch into the specimen. The intergranular region extended in for an additional seven or eight thousandths of an inch. Figs. 6 and 7 show some of these facets. They also show numerous opaque particles and only a few dimples. Fig. 6 shows some of the burnishing markings at the top and bottom (horizontal arrows show examples).

About 10 thousandths of an inch from the outer surface the fracture mode changed from almost totally intergranular to mixed intergranular and dimples as shown in Figs. 8-10. The remainder of the fracture surface was a mixture of intergranular fracture and dimples, such as those shown,

except for the small isolated patches of completely intergranular fracture in the macroscopically flat bottoms of holes and tops of "mesas" shown at low magnification in Fig. 3 and at high magnification in Fig. 11. Fig. 12 is a low magnification electron fractograph showing the collapsed sides of a "mesa". (Large elevation changes in replicas like these collapse due to the surface tension of the acetone when the replicas are placed onto grids and removed from the acetone.)

Figs. 13 and 14 are low magnification electron fractographs of selected portions of a replica taken from one of the NASA low-cycle fatigue fracture surfaces. This specimen underwent 13 cycles before fracture (1). These fractographs show two of the raised portions (between the arrows) found on this fracture surface (indicated by arrows in Fig. 4). Here the elevation differences were not enough to cause extensive collapsing of the replicas. No intergranular fracture was found associated with these raised portions - only plastic flow dimples and "ripples" indicative of large amounts of local plastic flow. No fatigue striations could be found.

CONCLUSIONS

The nose gear outer cylinder contained a small surface flaw approximately 5/32-inch long and about 10 thousandths of an inch deep before testing. The length of this flaw was

measured by the distance between the shear lips (Fig. 3). The depth was measured by the depth of the initial intergranular region. The opaque particles in Figs. 5 and 6 are similar to those seen previously on surface cracks exposed to heat treatment environment (e.g., during tempering).

The presence of the submerged cracks is not fully explained due to the lack of sufficient data (rates of load application during the test is one unknown factor). They were either formed due to quenching stresses during the heat treatment, due to residual stresses and hydrogen embrittlement during or after plating, or they grew during the test as a result of hydrogen embrittlement. The fact that these cracks became linked with the surface crack by mixed micro-void coalescence and intergranular separation, rather than by solely intergranular fracture during the test supports the view that they were present prior to the test. (4340 in this heat treated condition fractures by mixed grain boundary fracture and void coalescence to form dimples in plane strain tests in the absence of hydrogen.) The facts that they were found only near the fracture origin and that the piece underwent several loadings to the UTS before fracture support the view that they were formed during the test. These submerged cracks were oriented perpendicular to the length of the cylinder which coincides

with the stresses imposed during the test but not necessarily with the major stresses arising from quenching, or quenching and tempering. This supports the view that they were formed during the test. Regardless of their origin, the submerged cracks could significantly lower the stress necessary to cause fracture.

The presence of large secondary cracks that were found during the chromium stripping operation indicates that significant residual stresses were present in the fractured piece and therefore in the piece prior to plating and testing since no general necking of the piece occurred during testing. It is evident that these cracks were formed after the primary fracture by either hydrogen embrittlement or stress corrosion cracking since no shear lips could be found associated with them.

The burnished edge of the fracture origin between the shear lips are typical of mishandled fracture surfaces and are caused by bumping or rubbing the edge against another hard surface.

The shiny spots on the NASA low-cycle fatigue specimens fracture surface (Fig. 4) showed no periodic fatigue markings and no intergranular fracture. This surface was formed in the necked region of a smooth bar and therefore neither the test conditions nor the fracture surface are comparable to the nose-gear test and its fracture surface.

SUMMARY

The nose-gear outer cylinder fractured due to (1) the presence of a small surface crack and several small submerged cracks, all of which were intergranular, and (2) the high stresses imposed during the test. The presence of these cracks probably considerably reduced the number of cycles to failure in this specimen. The cracks were quite possibly, but not definitely, due to the presence of hydrogen and residual stresses during plating or during the test.

REFERENCE

1. "Fatigue Behavior of Materials Under Strain Cycling in Low and Intermediate Life Range", NASA TND-1574, Apr 1963.

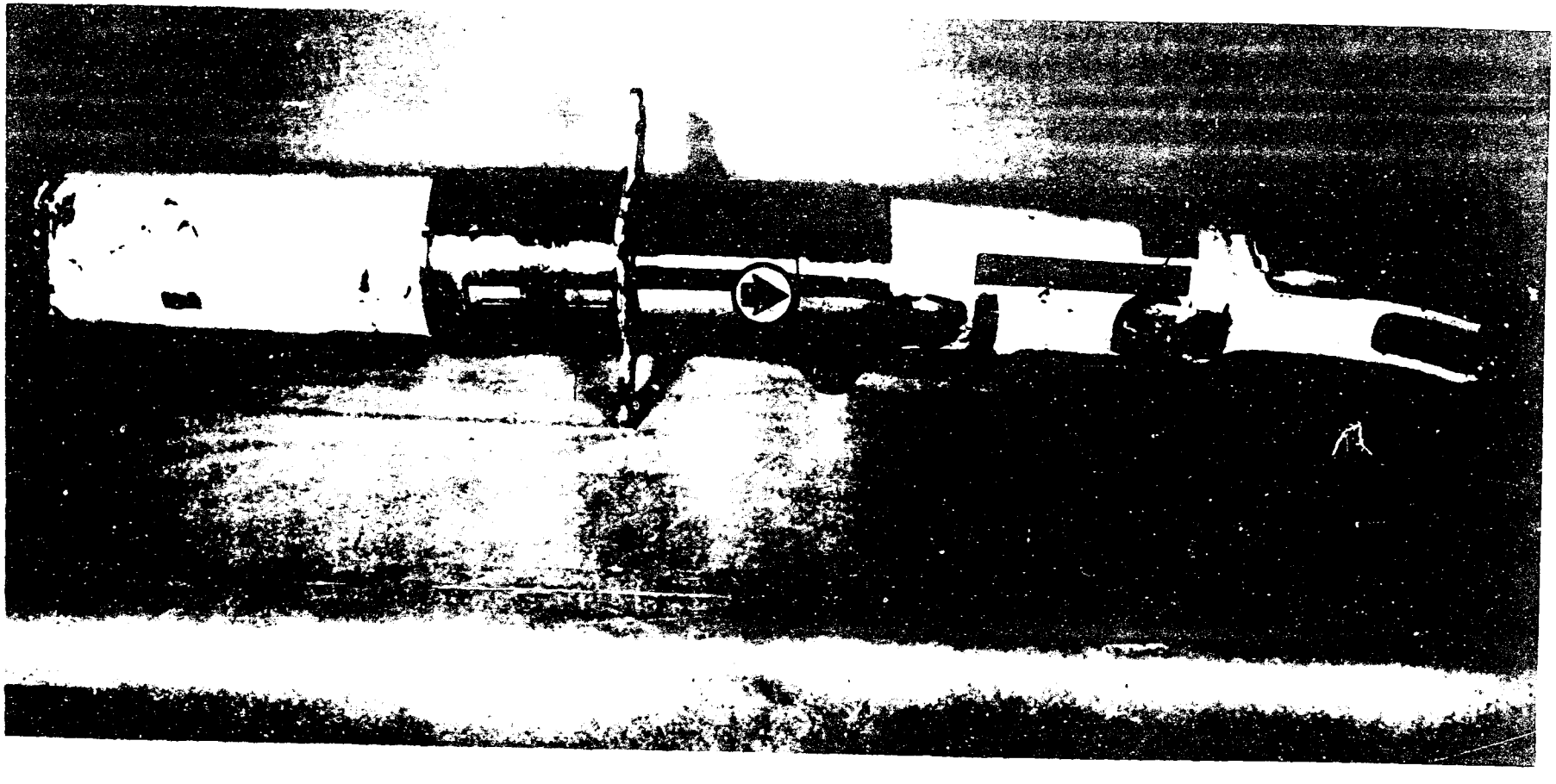

Fig. 1 - Laboratory tested C-141 nose gear outer cylinder, with arrow showing fracture origin. Photograph courtesy of Lockheed Aircraft Co.

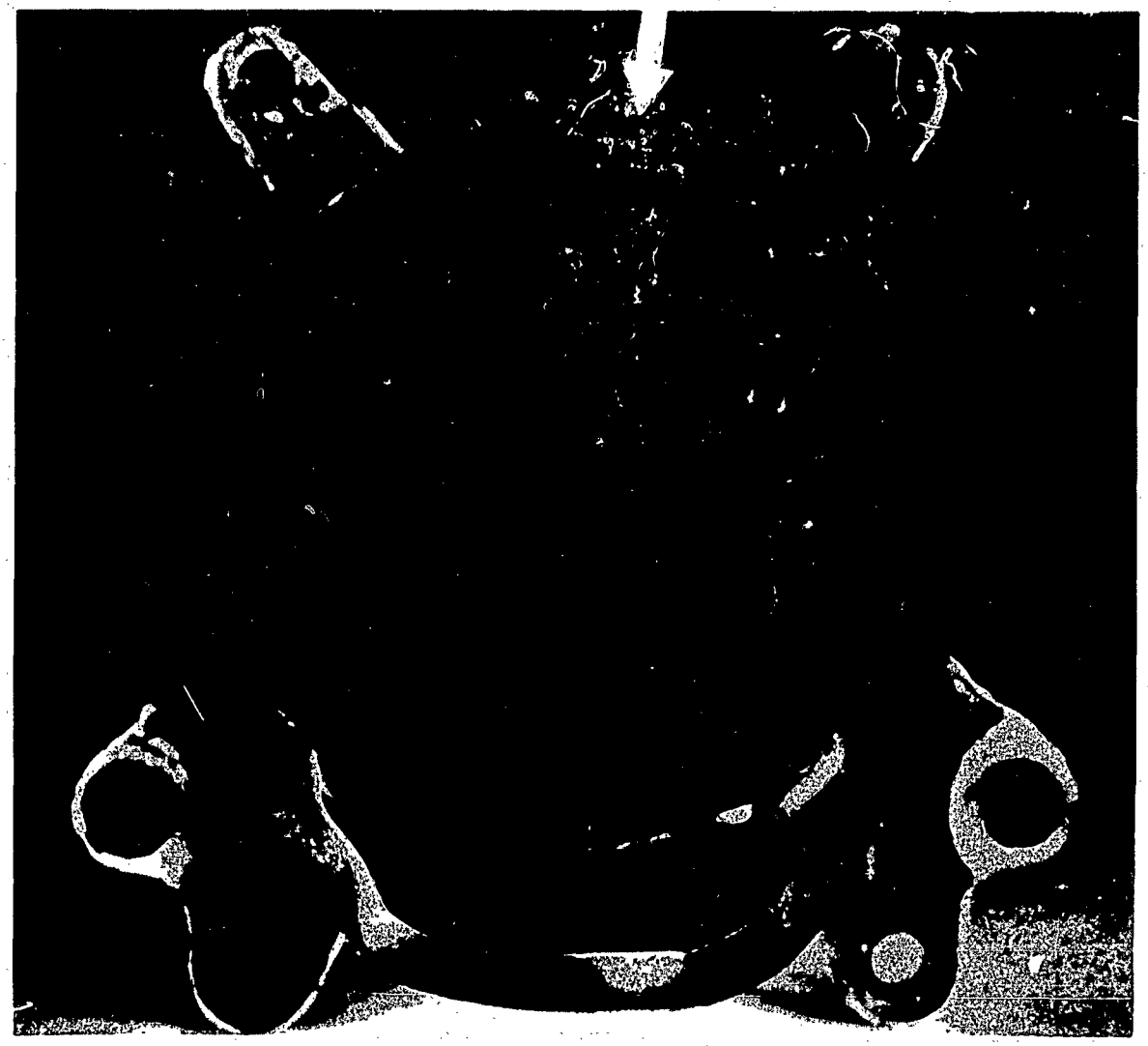

Fig. 2 - View of fracture surface with chevron markings and arrow pointing to the fracture origin. Approximately 3/4 X. Photograph courtesy of Lockheed Aircraft Co.

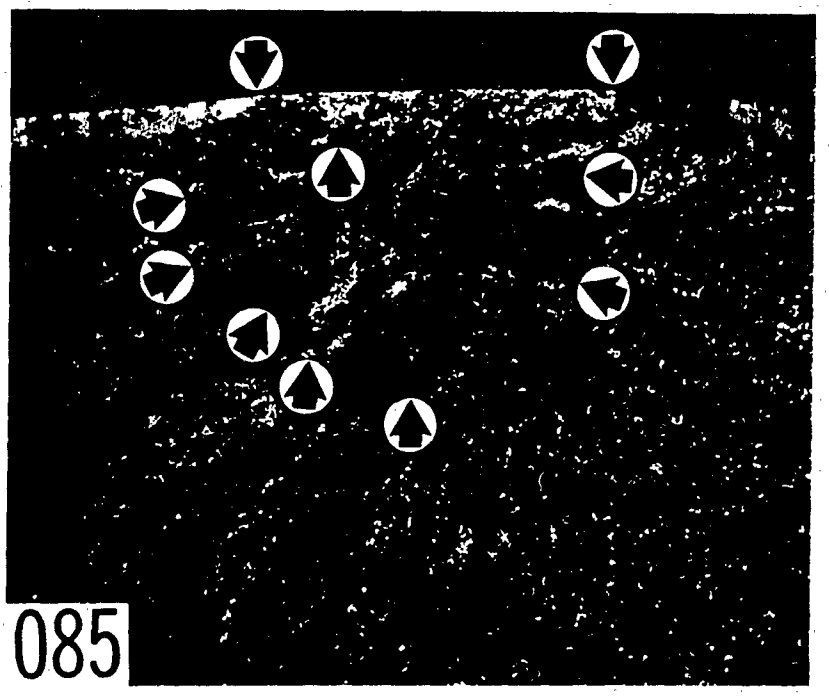

Fig. 3 - Higher magnification view of fracture initiation region. Two arrows at top show length of small surface crack present before the fracture. Other arrows indicate flat-topped hills or flat-bottomed holes. Approximately 14 X.

Fig. 4 - NASA low-cycle smooth-bar fatigue specimen that broke after 13 cycles. Arrows indicate shiny spots which were examined for fatigue striations. Approximately 10 X.

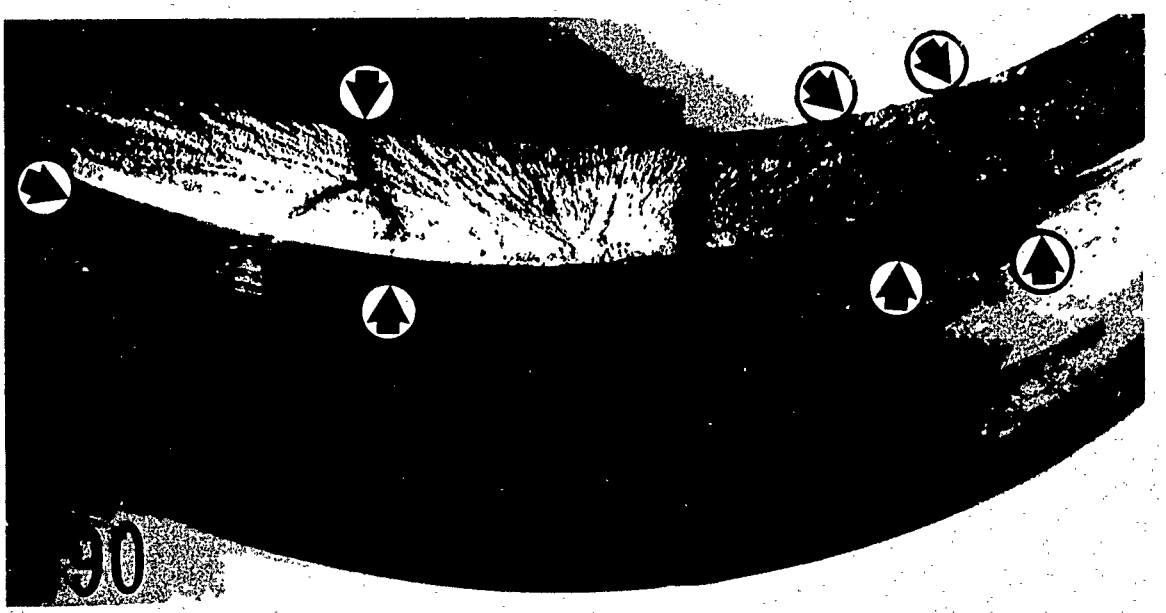

Fig. 5 - View of a portion of the fracture surface showing cracks between the arrows. Approximately 2 X.

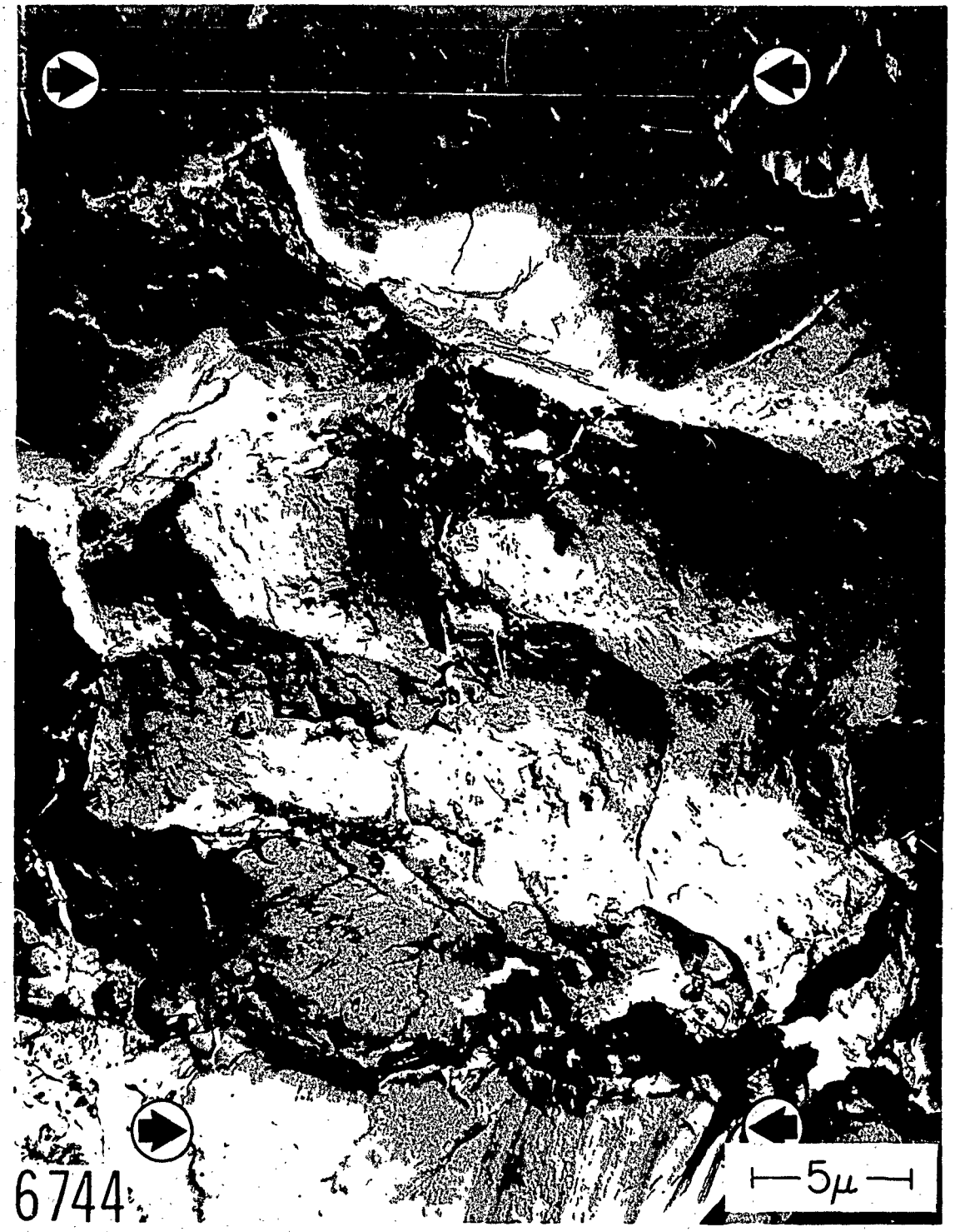

Fig. 6 - Burnishing markings (arrows), intergranular facets, and opaque particles on the surface of the surface crack where the fracture initiated. Two-stage palladium-shadowed carbon replica. 6000X.

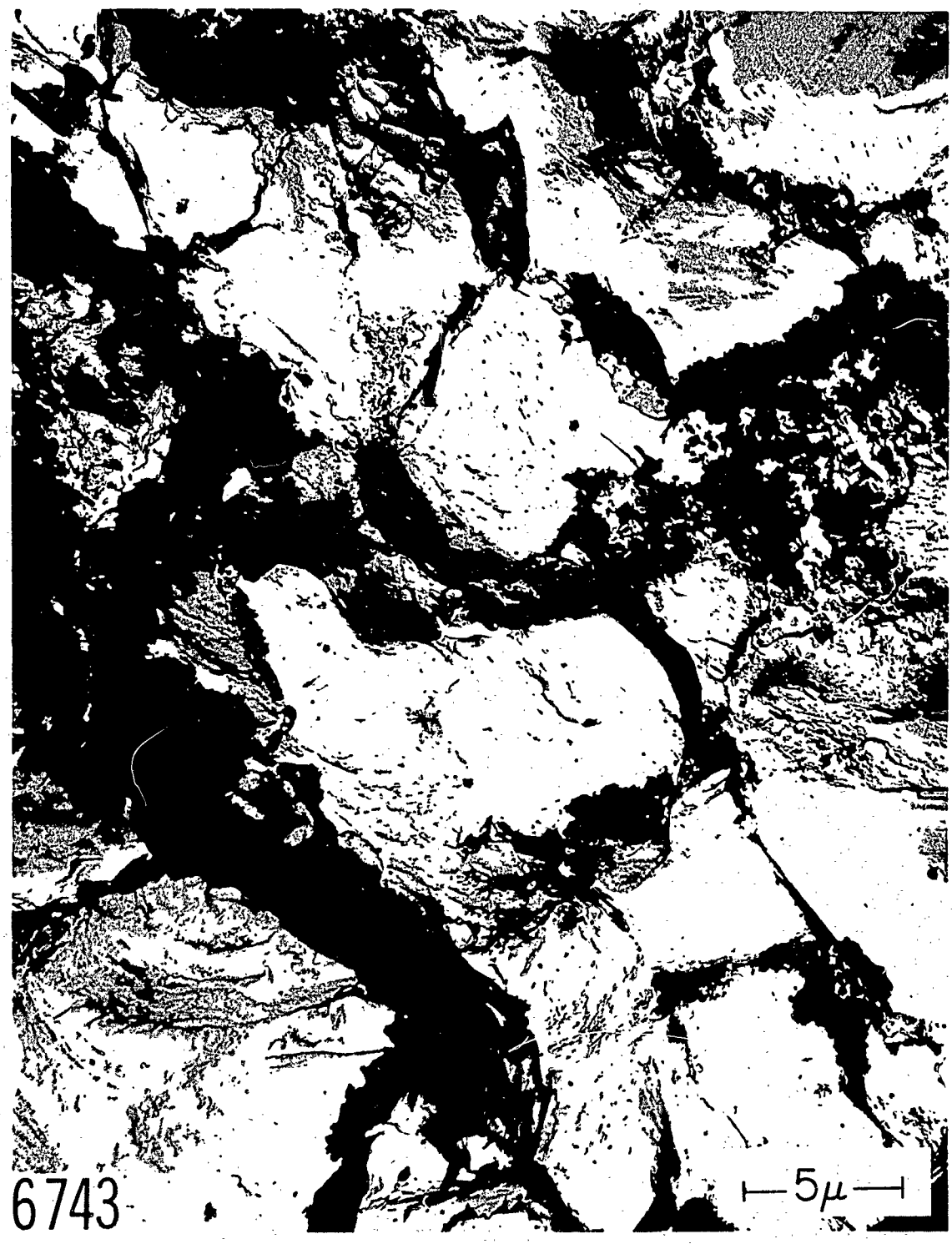

Fig. 7 - Grain facets and opaque particles on surface of shallow surface crack. Two-stage palladium-shadowed carbon replica. 6000X.

Fig. 8 - Mixed intergranular fracture and dimples typical of some plane-strain fracture surfaces in 4340 steel. View of fracture surface beneath the surface flaw. Other typical regions are shown in Figs. 8 and 9. Two-stage palladium-shadowed carbon replica. 6000X.

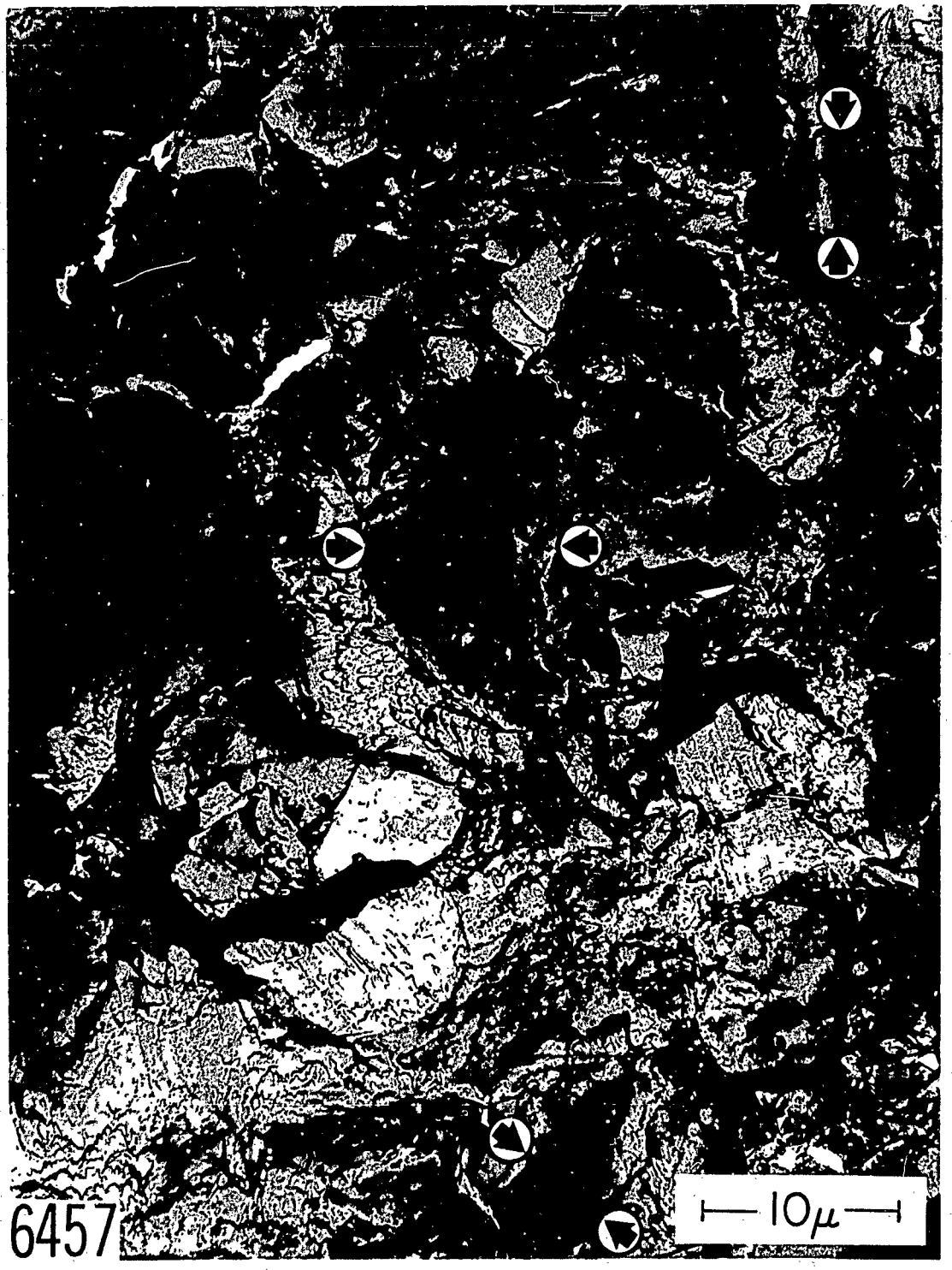

Fig. 9 - Lower magnification view of fracture surface below surface crack. Flat regions (examples shown between arrows), that are probably intergranular facets, are mixed with dimples. Again this is typical of simple overload plane strain fracture in 4340 steel with this heat treatment. Two-stage palladium-shadowed carbon replica. 3600X.

Fig. 10 - Another region below the surface crack which exhibits a different arrangement of mixed intergranular fracture and dimple. Two-stage palladium-shadowed carbon replica. 6000X.

Fig. 11 - Completely intergranular fracture typical of the surfaces at the bottoms of holes and tops of hills located immediately below the surface crack. Two-stage palladium-shadowed replica. Approximately 3000X.

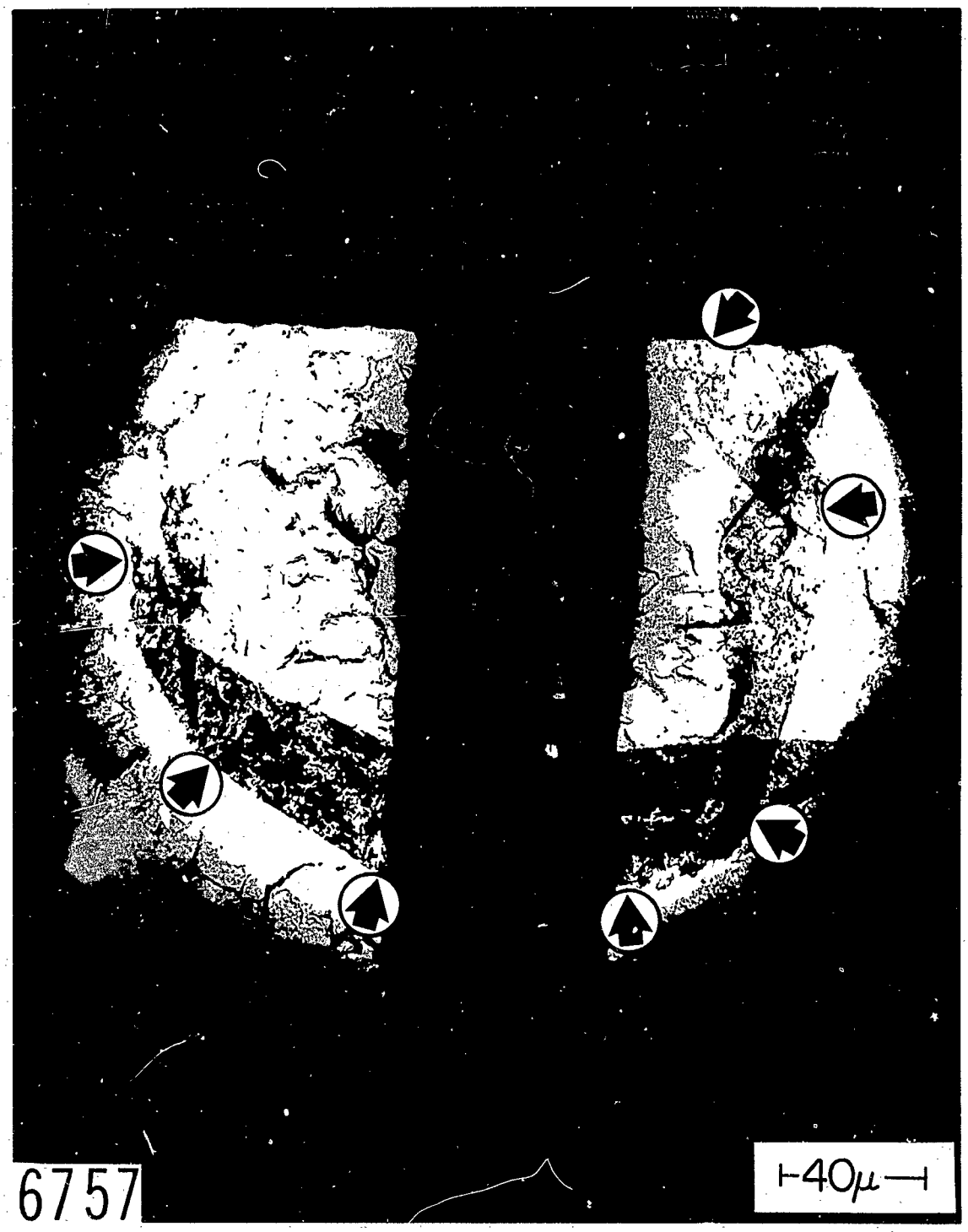

Fig. 12 - Collapsed replica (arrows) showing large and sudden elevation change between the plane of the major fracture and one of the truncated hills or one of the flat-bottomed holes. Two-stage carbon replica. 630 X.

Fig. 13 - One of the shiny spots (shown at lower magnification in Fig. 4) on a NASA low-cycle fatigue specimen. Local fracture initiation region is bounded by arrows. Two-stage palladium-shadowed carbon replica. 1800X.

Fig. 14 - Another of the shiny spots in the NASA low-cycle fatigue specimen. 2600X.